

Shortwave Aerosol Radiative Forcing from MODIS and CERES observations over the oceans

Sundar A. Christopher and Jiangleong Zhang

Department of Atmospheric Sciences, University of Alabama, Huntsville, USA

Received 25 January 2002; revised 1 March 2002; accepted 20 March 2002; published 18 September 2002.

[1] Using spatially and temporally collocated data sets from the Clouds and Earth's Radiant Energy System (CERES) and Moderate-Resolution Imaging Spectroradiometer (MODIS) instruments on the Terra satellite, a new strategy is presented for studying the Shortwave Aerosol Radiative Forcing (SWARF) over the global oceans. Using collocated data, for September 2000, the global averaged optical thickness ($\tau_{0.55}$) for cloud-free CERES pixels is 0.07 with a SWARF of -6 Wm^{-2} . The $\tau_{0.55}$ and SWARF values derived from two independent instruments are in excellent agreement with the following relationship: $\text{SWARF} = 0.35 - 105.34\tau_{0.55} + 61.47\tau_{0.55}^2$ ($0 \leq \tau_{0.55} \leq 0.7$) Wm^{-2} . The synergistic use of the MODIS and CERES data sets can be used to provide independent estimates of SWARF, and can be used as a validation tool for studies that attempt to model the role of aerosols on climate. **INDEX TERMS:** 0305 Atmospheric Composition and Structure: Aerosols and particles (0345, 4801); 3359 Meteorology and Atmospheric Dynamics: Radiative processes; 3360 Meteorology and Atmospheric Dynamics: Remote sensing. **Citation:** Christopher, S. A., and J. Zhang, Shortwave Aerosol Radiative Forcing from MODIS and CERES observations over the oceans, *Geophys. Res. Lett.*, 29(18), 1859, doi:10.1029/2002GL014803, 2002.

1. Introduction

[2] Aerosols play a key role on the radiation balance of the earth-atmosphere system. The study of the radiative effects of tropospheric aerosols including mineral dust, organic carbon, black carbon, and sulfate have proved to be a challenging task due to the spatial and temporal variability of aerosol distribution and its properties. Current estimates of Shortwave Aerosol Radiative Forcing (SWARF) for biomass burning and fossil fuel aerosols range from -0.1 to -0.5 Wm^{-2} and -0.1 to -1.0 Wm^{-2} respectively, and the sign and magnitude of the radiative effect is still uncertain [IPCC, 2001]. Typical approaches for studying the radiative forcing of aerosols include: (1) Use of radiative transfer equations to calculate radiative forcing of optically thin aerosols [e.g., Penner *et al.*, 1992]; (2) Use of General Circulation Models (GCM) [e.g., Hansen *et al.*, 1998]; and (3) Use of satellite-derived aerosol distributions and aerosol optical thickness (τ) to calculate the effect of aerosols in radiative transfer models [e.g., Christopher and Zhang, 2002]. Recently, several studies have shown the potential of satellite-retrieved top-of-the-atmosphere (TOA) fluxes to examine the radiative effect of aerosols. Christopher *et al.*

[2000] studied the radiative effect of biomass burning over Central America by using collocated Clouds and Earth's Radiant Energy System (CERES) and Visible Infrared Scanner (VIRS) measurements from the Tropical Rainfall Measuring Mission (TRMM) platform. Using VIRS and CERES data, Loeb and Kato [2002] have extended this approach to study the direct radiative forcing of aerosols over the oceans. This approach of using combined satellite measurements provides an independent method for studying the impact of aerosols on climate. NASA's suite of well-calibrated sensors on the Terra satellite provides an unprecedented opportunity to study the effect of aerosols on climate. In this paper, we estimate the SWARF in cloud free regions over the global oceans using a combination of CERES and Moderate-Resolution Imaging Spectroradiometer (MODIS) data sets from Terra.

2. Data and Methodology

[3] Three data sets are used in this study; the MODIS Level 2 (MOD04) daily aerosol product [Tanré *et al.*, 1997]; the MODIS Level 2 daily (MOD06) cloud product [Ackerman *et al.*, 1998], and the pixel level CERES ES-8 at a spatial resolution of 30 km at nadir [Wielicki *et al.*, 1996]. The MOD04 and MOD06 provide aerosol and cloud properties and CERES ES-8 data provides TOA SW fluxes. The CERES ES-8 data contains broadband TOA SW (0.3–5 μm) and longwave (5.0–50.0 μm) fluxes that are inverted from measured radiances using Angular Distribution Models (ADM's) developed for the Earth Radiation Budget Program (ERBE) program [Wielicki *et al.*, 1996].

[4] Using measured radiances at 500 m spatial resolution from six bands between 0.55–2.1 μm , the primary aerosol products retrieved by the MODIS algorithm include spectral aerosol optical thickness, the aerosol effective radius (r_e), and the fraction of the total optical thickness contributed by the sub-micron size mode aerosol [Tanré *et al.*, 1997]. These aerosol properties are then reported at 10 km spatial resolution in the MOD04 data. Based on theoretical sensitivity studies, the uncertainties in $\tau_{0.55}$ retrievals are estimated to be $\pm 0.05 \pm 0.05\tau_{0.55}$ over ocean [Tanré *et al.*, 1997]. The MODIS aerosol optical thickness product has been validated against sunphotometer derived values over oceans and recent results have confirmed that the MODIS algorithm over ocean areas is performing within the expected accuracy [Remer *et al.*, 2002].

[5] The MOD06 product provides cloud top parameters, such as cloud top pressure and cloud top temperature, at 5 km resolution and cloud optical parameters, such as cloud optical thickness and cloud effective radius, at 1 km resolution [Ackerman *et al.*, 1998]. The MOD06 data also provides cloud fraction at both 1 and 5 km resolution. In

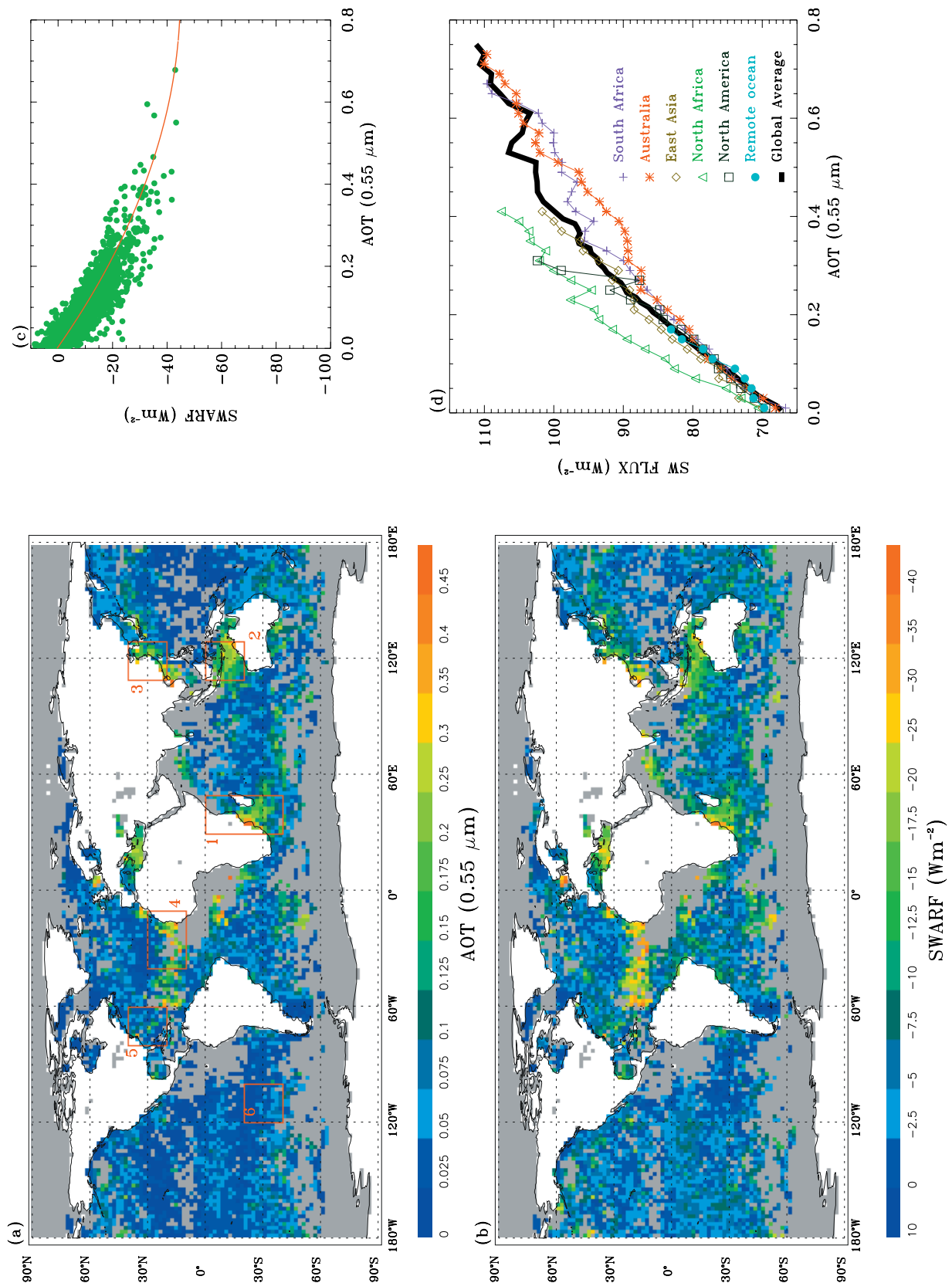


Figure 1. (a) Spatial distribution of MODIS $\tau_{0.55}$ over the global ocean for cloud-free CERES pixels. Missing data for cloud cover shown in gray and the six selected regions (see text) are shown in red boxes. *Remer et al.* [2002] show the full range of MODIS $\tau_{0.55}$. (b) Spatial distribution of CERES-derived SWARF over global ocean. (c) MODIS retrieved $\tau_{0.55}$ versus CERES SWARF. A second-order polynomial fit is shown by the solid red line. (d) Averaged MODIS $\tau_{0.55}$ vs. CERES SW fluxes for six selected regions. Solid black line shows the globally averaged values.

Table 1. Summary of MODIS and CERES derived values for the six selected regions

Region	Latitude degrees	Longitude degrees	No. ^a	SWARF Wm ⁻²	τ (0.55 μ m)	r_c μ m
Australia	20S – 0	110E – 130E	19947	-13.37	0.172	0.43
East Asia	20N – 40N	110E – 130E	2479	-12.43	0.143	0.40
North Africa	10N – 30N	40W – 10W	4709	-12.56	0.114	1.25
North America	20N – 40N	80W – 60W	3678	-8.02	0.067	1.13
South Africa	40S – 0	30E – 50E	20075	-12.66	0.139	0.81
Remote Ocean	40S – 20S	120W – 100W	4844	-1.73	0.039	1.65

^aNumber of CERES pixels.

this study, we take each CERES footprint and collocate the 5 km MOD06 data to identify cloud-free regions. For these cloud free regions, we obtain aerosol properties from the MOD04 data. Twenty-nine days of global CERES and MODIS (MOD04 and MOD06) data in September 2000 were used in this study (CERES ES-8 data from September 17th was unavailable) and is roughly equivalent to about 500GB of data.

[6] On Terra, there are two CERES instruments. One instrument operates in a cross track scan mode similar to that of the ERBE scanner while the second instrument operates in a biaxial scan mode to provide new angular flux information [Wielicki *et al.*, 1996]. In this study, only the cross track scan mode data is used. The CERES pixels that are labeled as “clear ocean” by the CERES ES-8 data were first selected. However, due to the large footprint of the CERES scanner, these pixels could still have some cloud contamination. To eliminate these cloud effects, the MOD06 data is collocated with the CERES data and only those CERES pixels with a 0% cloud fraction as identified by the MOD06 data were used. By using such a stringent cloud screening criteria, it is possible that thick aerosol plumes are rejected in the analysis.

[7] The SWARF¹ at the top of the atmosphere (TOA) is defined as the difference between clear (F_{clr}) and aerosol (F_{aer}) fluxes [Christopher *et al.*, 2000]. In this study, F_{clr} and F_{aer} were averaged over $2^\circ \times 2^\circ$ (latitude \times longitude) bins. The F_{aer} values are obtained by averaging the cloud free CERES ES-8 data within a $2^\circ \times 2^\circ$ bin. However, F_{clr} is more difficult to obtain because when aerosol loading is low, satellite imagers are not effective in detecting aerosols. To obtain F_{clr} values, we use cloud free CERES pixels that have $\tau_{0.55} < 0.02$, as determined by the MODIS data. Due to this assumption, our first order estimation shows that the uncertainties in F_{clr} is on the order of 1Wm^{-2} .

3. Results and Discussion

[8] Figures 1a and 1b show the global distribution of MODIS-retrieved $\tau_{0.55}$ and CERES-derived SWARF for collocated cloud-free MOD04 and CERES ES-8 data over ocean areas. We emphasize that the aerosol optical thickness shown in Figure 1a is reported for cloud-free CERES pixels. Therefore some aerosol features are not seen due to the possible cloud contamination and stringent cloud screening procedure (see section 2). For example, smoke from South Africa and pollution from the Indian subcontinent that is seen in Remer *et al.* [2002] is not seen in Figure 1a due to

cloud contamination or misidentification of aerosol pixels as being cloudy. The spatial distribution of $\tau_{0.55}$ and SWARF derived from two independent sets of measurements are remarkably consistent. Missing data shown in gray is often due to persistent cloud coverage often observed over the West Coast of South America and Africa and over the Inter Tropical Convergence Zone (ITCZ). The spatial distribution of $\tau_{0.55}$ is consistent with previously reported values [Remer *et al.*, 2002]. The regions with $\tau_{0.55}$ values greater than 0.15 are dominated by: (1) dust plumes over the Atlantic Ocean and the Mediterranean sea originating from North Africa; (2) biomass burning aerosols over the Indian Ocean and South Atlantic Ocean from South Africa and smoke aerosols over the Indian Ocean from Australia; (3) Pollutant aerosols from East Asia to the North Pacific Ocean and from Europe to the North Atlantic Ocean. The averaged $\tau_{0.55}$ and SWARF values are 0.07 (Figure 1a) and -6Wm^{-2} (Figure 1b) respectively for cloud-free regions as observed by CERES. Superimposed on Figure 1a are six boxes, which represent selected regions over the ocean and are labeled after the closest aerosol source regions (except Remote Ocean). The six areas are (1) South Africa (SA) ($0-40^\circ\text{S}$, $30-50^\circ\text{E}$), (2) Australia (AUS) ($0-20^\circ\text{S}$, $110-130^\circ\text{E}$), (3) East Asia (EA) ($20-40^\circ\text{N}$, $110-130^\circ\text{E}$), (4) North Africa (NAF) ($10-30^\circ\text{N}$, $10-40^\circ\text{W}$), (5) North America (NAM) ($20-40^\circ\text{N}$, $60-80^\circ\text{W}$), and (6) Remote Ocean (RO) ($20-40^\circ\text{S}$, $100-120^\circ\text{W}$).

[9] Figure 1c shows the relationship between MODIS-retrieved $\tau_{0.55}$ versus the CERES-derived SWARF. The aerosol optical thickness and SWARF derived from two independent methods are highly correlated. The SWARF is most sensitive to $\tau_{0.55}$ changes when $\tau_{0.55}$ is low and less sensitive to $\tau_{0.55}$ changes when the aerosol loading is high. For example, a change in $\tau_{0.55}$ from 0 to 0.05 causes a change in SWARF of -5.1Wm^{-2} and a change in $\tau_{0.55}$ from 0.45 to 0.5 causes a change in SWARF of -2.3Wm^{-2} . A second order polynomial fit through data points yields the following relationship: $\text{SWARF} = 0.35 - 105.34\tau_{0.55} + 61.47\tau_{0.55}^2$ ($0 \leq \tau_{0.55} \leq 0.7$) Wm^{-2} . However, this relationship was developed for only one month of data and may change significantly for other months.

[10] Figure 1d shows the $\tau_{0.55}$ versus the cloud-free SW flux for the six selected regions. The globally averaged value is indicated by the solid red line. When the $\tau_{0.55}$ is less than 0.2, the relationship between SWARF and $\tau_{0.55}$ is similar among the different regions (except for NAF) because when aerosol loading is low, the background aerosols are major contributors to SWARF. The NAF region dominated by dust aerosols is most efficient in reflecting incoming solar energy when compared with other regions. The aerosols from the SA and AUS source regions have

¹SWARF = $F_{\text{clr}} - F_{\text{aer}}$, where F_{aer} is the TOA SW flux in aerosol regions, and F_{clr} is the TOA clear sky flux.

lower SWARF values when $\tau_{0.55}$ is greater than 0.2. The slopes of $\tau_{0.55}$ vs. SW flux for the SA and AUS regions are very similar, which implies that the aerosols in these two regions have similar radiative properties where the dominant aerosol type is from biomass burning. Recent studies show that the single scattering albedo (ω_0) of dust and smoke aerosols at 0.64 μm is 0.97 [Kaufman *et al.*, 2001] and 0.86 [Reid *et al.*, 1998] respectively. The higher ω_0 values of dust leads to higher TOA SW values when compared with SW flux values for regions dominated by biomass burning and pollutant aerosols. The slope of $\tau_{0.55}$ vs. SW flux for the EA region is between that of dust and smoke regions. The dominant aerosol type is from industrial pollution that has different aerosol radiative characteristics when compared with dust and smoke aerosols.

[11] Table 1 summarizes the results for the six regions. The lowest averaged $\tau_{0.55}$ of 0.039 is observed over the RO region with a SWARF value of -1.73 Wm^{-2} . The highest averaged $\tau_{0.55}$ of 0.17 is found near Australia with a SWARF value of -13.37 Wm^{-2} . The EA and SA regions have similar $\tau_{0.55}$ and SWARF values. However, the NAF region has a SWARF value of -12.56 Wm^{-2} , that is similar to SWARF values over EA and SA regions with a lower $\tau_{0.55}$ of about 0.114. This indicates the differences in aerosol radiative characteristics between regions dominated by dust (NAF), biomass burning (SA), and pollutant aerosols (EA). The aerosol effective radii (r_e) are 1.25 and 1.65 μm for NAF and RO regions respectively. The predominant aerosol type in NAF is dust aerosol with r_e on the order of 1.5–2.5 μm [Kaufman *et al.*, 2001]. The dominant aerosol type over the RO is sea salt, that has a similar or even larger peak effective radius when compared with dust aerosols [Andreas, 1998]. In comparison, the r_e values are smaller for SA, AUS, and EA regions because aerosols in these regions are dominated by either smoke or pollutant aerosols with r_e values on the order of 0.1–0.2 μm [Kaufman *et al.*, 2001; Reid *et al.*, 1998].

4. Conclusions

[12] This study shows a new strategy for studying the effect of aerosols on the radiation balance of the earth-atmosphere system through synergistic use of multiple instruments on the same satellite. However, the uncertainties involved in this study should be carefully examined in future studies. One of the uncertainties that arise from this approach is the lack of ADM's for aerosols. New strategies for developing ADM's for aerosols must be developed as a function of aerosol type and optical thickness. The biaxial scan mode data from CERES on Terra can be used to develop such ADM's. Other sources of uncertainty include estimation of F_{clr} in persistent cloudy areas and the effect of surface conditions such as wind speed. The focus of this paper was to examine the global aerosol direct radiative forcing over ocean for cloud free conditions. Averaged over

the entire month, for cloud-free CERES pixels, the $\tau_{0.55}$ is 0.07 and SWARF is -6 Wm^{-2} . This is a first step towards the study of global aerosol radiative forcing using satellite measurements. The next challenging step is to extend this work over land regions where the surface effects play an important role. The strengths of other instruments such as the Multi-angle Imaging SpectroRadiometer (MISR) with several view angles can also be utilized to reduce the uncertainties in SWARF.

[13] **Acknowledgments.** This research was partially supported by NASA grant NCC8-200 under the Global Aerosol Climatology Project. The CERES data were obtained from the NASA Langley Research Center Atmospheric Sciences Data Center and the MODIS data were obtained through the Goddard Space Flight Center Data Center. We also thank the CERES science team for providing the CERES point spread function and geolocation information.

References

- Ackerman, S. A., K. I. Strabala, W. P. Menzel, R. A. Frey, C. C. Moeller, and L. E. Gumley, Discriminating clear sky from clouds with MODIS, *J. Geophys. Res.*, 103, 32,141–32,157, 1998.
- Andreas, E. L., A new sea spray generation function for wind speeds up to 32 ms^{-1} , *J. Phys. Oceanogr.*, 28, 2175–2184, 1998.
- Christopher, S. A., and J. Zhang, Daytime variation of shortwave direct radiative forcing of biomass burning aerosols from GOES 8 imager, *J. Atmos. Sci.*, 59, 681–691, 2002.
- Christopher, S. A., J. Chou, J. Zhang, X. Li, and R. M. Welch, Shortwave direct radiative forcing of biomass burning aerosols estimated from VIRS and CERES, *Geophys. Res. Lett.*, 27, 2197–2200, 2000.
- Hansen, J., M. Sato, A. Lacis, R. Ruedy, I. Tegen, and E. Matthews, Climate forcings in the Industrial era, *Proc. Natl. Acad. Sci.*, 95, 12,753–12,758, 1998.
- Intergovernmental Panel on Climate Change (IPCC), Climate change 2001, The scientific basis, Cambridge University Press, 881 pp, 2001.
- Kaufman, Y. J., D. Tanré, O. Dubovik, A. Karnieli, and L. A. Remer, Absorption of sunlight by dust as inferred from satellite and ground-based remote sensing, *Geophys. Res. Lett.*, 28, 1479–1482, 2001.
- Loeb, N. G., and S. Kato, Top-of-Atmosphere direct radiative effect of aerosols from the Clouds and the Earth's Radiant Energy System Satellite instrument (CERES), *J. Climate*, 15, 1474–1484, 2002.
- Penner, J. E., R. E. Dickinson, and C. A. O'Neill, Effects of aerosol from biomass burning on the global radiation budget, *Science*, 256, 1432–1434, 1992.
- Reid, J. S., P. V. Hobbs, R. J. Ferek, D. R. Blake, J. V. Martins, M. R. Dunlap, and C. Liousse, Physical, chemical and optical properties of regional hazes dominated by smoke in Brazil, *J. Geophys. Res.*, 103, 32,059–32,080, 1998.
- Remer, L. A., D. Tanré, Y. J. Kaufman, C. Ichoku, S. Mattoo, R. Levy, D. A. Chu, B. N. Holben, O. Dubovik, A. Smirnov, J. V. Martins, R. R. Li, and Z. Ahmad, Validation of MODIS aerosol retrieval over ocean, *Geophys. Res. Lett.*, in press, 2002.
- Tanré, D., Y. J. Kaufman, M. Herman, and S. Mattoo, Remote sensing of aerosol properties over oceans using the MODIS/EOS spectral radiances, *J. Geophys. Res.*, 102, 16,971–16,988, 1997.
- Wielicki, B. A., B. R. Barkstrom, E. F. Harrison, R. B. Lee III, G. L. Smith, and J. E. Cooper, Clouds and the Earth's Radiant Energy System (CERES): An Earth observing system experiment, *Bull. Am. Meteorol. Soc.*, 77, 853–868, 1996.

S. A. Christopher and J. Zhang, Department of Atmospheric Sciences, NSSTC, University of Alabama in Huntsville, 320 Sparkman Drive, Huntsville, AL 35806, USA. (sundar@nsstc.uah.edu)